



Research article

Design, synthesis, and cytotoxic evaluation of quinazoline derivatives bearing triazole-acetamides



Keyvan Pedrood^a, Fahimeh Taayoshi^b, Ali Moazzam^a, Aida Iraj^{c,d}, Ali Yavari^a, Samira Ansari^e, Sayed Mahmoud Sajjadi-Jazi^a, Mohammad Reza Mohajeri-Tehrani^a, Nadia Garmsiri^f, Vahid Haghpanah^a, Meysam Soleymanibadi^g, Bagher Larijani^a, Haleh Hamedifar^{e,h}, Neda Adibpour^{b,**}, Mohammad Mahdavi^{a,*}

^a Endocrinology and Metabolism Research Center, Endocrinology and Metabolism Clinical Sciences Institute, Tehran University of Medical Sciences, Tehran, Iran

^b Department of Medicinal Chemistry, School of Pharmacy, Zanjan University of Medical Sciences, Zanjan, Iran

^c Stem Cells Technology Research Center, Shiraz University of Medical Sciences, Shiraz, Iran

^d Central Research Laboratory, Shiraz University of Medical Sciences, Shiraz, Iran

^e CinnaGen Medical Biotechnology Research Center, Alborz University of Medical Sciences, Karaj, Iran

^f Department of Biology, Payame Noor University (PNU), P.O.Box 19395-4697, Tehran, Iran

^g Department of Pharmaceutical Biotechnology, School of Pharmacy, Hamadan University of Medical Science Hamadan, Iran

^h CinnaGen Research and Production Co., Alborz, Iran

ARTICLE INFO

Keywords:

Anticancer activity
Click chemistry
Docking
Quinazoline

ABSTRACT

A novel series of quinazoline-based agents bearing triazole-acetamides **8a-l** were designed and synthesized. All the obtained compounds were tested for *in vitro* cytotoxic activities against three human cancer cell lines named HCT-116, MCF-7, and HepG2, as well as a normal cell line WRL-68 after 48 and 72 h. The results implied that quinazoline-oxymethyltriazole compounds exhibited moderate to good anticancer potential. The most potent derivative against HCT-116 was **8a** (X = 4-OCH₃ and R = H) with IC₅₀ values of 10.72 and 5.33 μM after 48 and 72 h compared with doxorubicin with IC₅₀ values of 1.66 and 1.21 μM, respectively. The same trend was seen in the HepG2 cancerous cell line in which **8a** recorded the best results with IC₅₀ values of 17.48 and 7.94 after 48 and 72 h, respectively. The cytotoxic analysis against MCF-7 showed that **8f** with IC₅₀ = 21.29 μM (48 h) exhibited the best activity, while compounds **8k** (IC₅₀ = 11.32 μM) and **8a** (IC₅₀ = 12.96 μM), known as the most effective cytotoxic agents after 72 h. Doxorubicin as positive control exhibited IC₅₀ values of 1.15 and 0.82 μM after 48 and 72 h, respectively. Noteworthy, all derivatives showed limited toxicity against the normal cell line. Moreover, docking studies were also presented to understand the interactions between these novel derivatives and possible targets.

* Corresponding author.

** Corresponding author.

E-mail addresses: n.adibpor@zums.ac.ir (N. Adibpour), momahdavi@sina.tums.ac.ir (M. Mahdavi).

<https://doi.org/10.1016/j.heliyon.2023.e13528>

Received 15 September 2022; Received in revised form 27 January 2023; Accepted 1 February 2023

Available online 4 February 2023

2405-8440/© 2023 Published by Elsevier Ltd.

This is an open access article under the CC BY-NC-ND license

(<http://creativecommons.org/licenses/by-nc-nd/4.0/>).

1. Introduction

Cancer is a multifactorial disease known as the uncontrolled growth of abnormal cells in a body that can infiltrate and destroy normal body tissue [1]. Cancer is expected to be one of the leading causes of death, affecting the lives of millions of people around the world. According to a report on the global burden of cancer worldwide, there were 18.1 million new cancer cases and 9.6 million cancer deaths in 2018 [2].

There are six common hallmarks of cancer: sustaining proliferative signaling, evading growth suppressors, resisting cell death, enabling replicative immortality, inducing angiogenesis, and activating invasion and metastasis [3,4]. Regarding the significant improvement in the pathogenesis of many types of cancer, various management and treatment strategies have been proposed, including novel chemotherapeutic, antimetastasis, therapeutic microRNA agents, immunotherapy, targeted therapy, hormonal therapy, and in some cases, surgical operations [5–8]. However, despite the continuous advance in medicine, the cancer burden continues to grow globally. It seems that the development of potent anticancer agents is considered vital.

In recent decades, quinazoline as a heterocyclic pharmacophore has become key building block in a variety of biological active agents as anti-fungal [9], anti-human immunodeficiency virus (HIV) [10], anti-influenza A virus (IAV) [11], and anti-hepatitis C virus (HCV) [12], antibacterial [13–17] as well as cytotoxic agents [18–20]. The Food and Drug Administration (FDA) approved quinazoline-based anticancer drugs, including gefitinib, erlotinib, lapatinib, afatinib, and vandetanib (Fig. 1) [21]. The other reason to increase research on this potentially privileged scaffold is its economical and convenient synthetic method [22].

1,2,3-Triazoles also demonstrated a prominent place in drug discovery due to their facile synthesis through click reaction [28] as well as wide biological profiles including antibacterial [23–25], anti-diabetes [26,27], anti-Alzheimer [28], and anticancer activities [29–31]. Triazoles ring can form various interactions such as hydrogen, hydrophobic, dipole-dipole bonds, and van der Waals forces with different biological targets that induce diverse pharmaceutical properties [32].

Recently some authors demonstrated anticancer agents derived from quinazoline derivatives (Fig. 2.). In detail, a series of 2-thioquinazolinone derivatives were synthesized and evaluated as anticancer agents. Compound A, the most active member of this study, showed IC_{50} values of 4.47, 7.55, and 4.04 μM against HCT-116, HeLa, and MCF-7 cell lines, respectively. Compound A also exhibited potent multi-target inhibitory activities against Hsp90, EGFR, VEGFR-2, and Topoisomerase-2 with IC_{50} values in the nanomolar range; 25.07, 38.5, 126.95 and 25.85 nm, respectively [33]. Another study showed that the proliferation rate of PC3 cells was reduced by compound B with an IC_{50} value of 17.7 μM compared to sorafenib with an IC_{50} value of 17.3 μM . Derivative B also underwent apoptotic effects with moderate inhibition of the growth of blood vessels [34]. GonçalvesNunes et al. also synthesized 4-aminoquinazoline derivatives bearing a 1,2,3-triazole core. Evaluation on BT-20 revealed that compound C had $IC_{50} = 24.6 \mu\text{M}$ against BT-20 cells. Western blot analysis exhibited a drastic decrease in the levels of ERK1/2 and p-STA3 in BT-20 cells under compound C incubation [35]. Moreover, compound D exerted high cytotoxicity against MDA-MB-231 ($IC_{50} = 3.21 \mu\text{M}$) and HT-29 ($IC_{50} = 7.23 \mu\text{M}$) cell lines. According to flow cytometric analysis, compound D induced G0/G1 phase of cell cycle arrest in a dose-dependent manner with typical apoptotic morphology like cell shrinkage, chromatin condensation and horseshoe-shaped nuclei formation [36]. AZD2932 (compound E) with quinazoline-triazole structure exhibited anticancer activity and inhibited VEGFR-2 with an $IC_{50} = 8 \text{ nM}$ regarded as a potential inhibitor of angiogenesis [37].

The current work continues our effort to design and synthesize novel cytotoxic agents [38,39]. This pursuit is inspired by introducing the effective quinazoline core, which was reported as a potent anticancer moiety, into the aryl-triazole group as an efficient

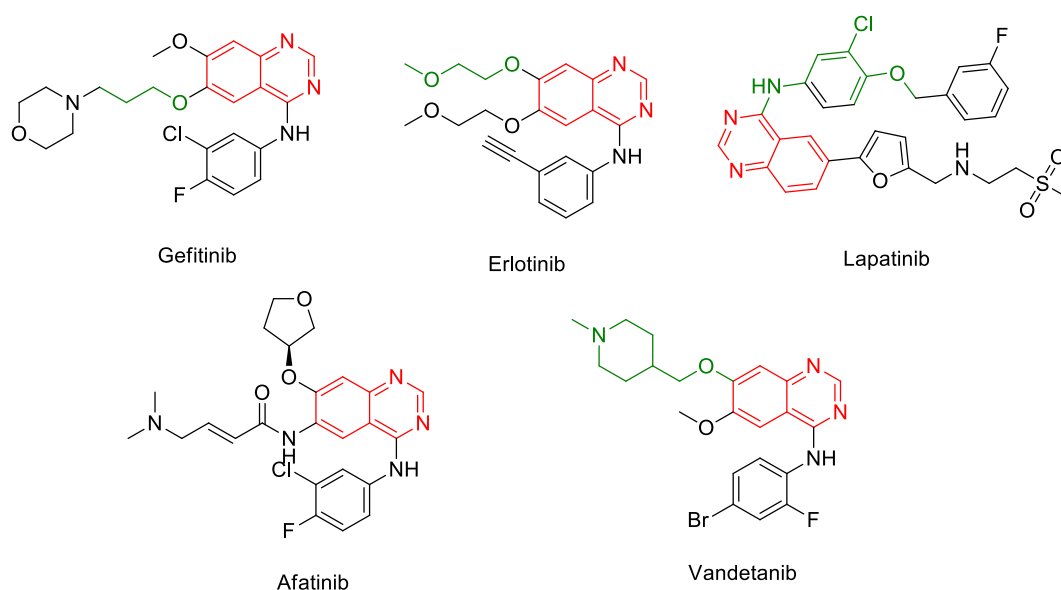


Fig. 1. Structure of some reported anticancer agents bearing quinazoline moiety.

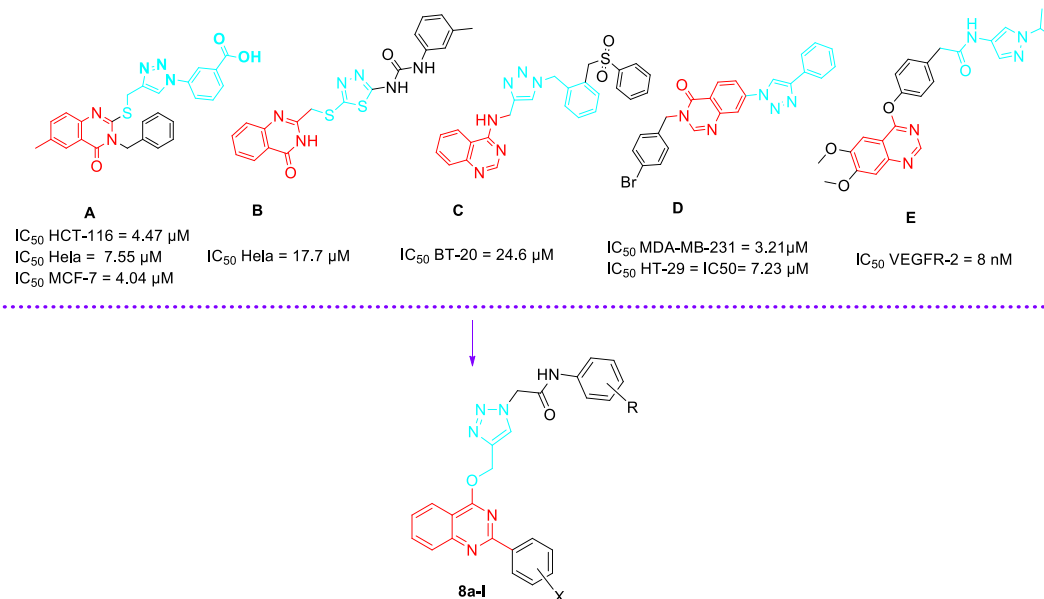
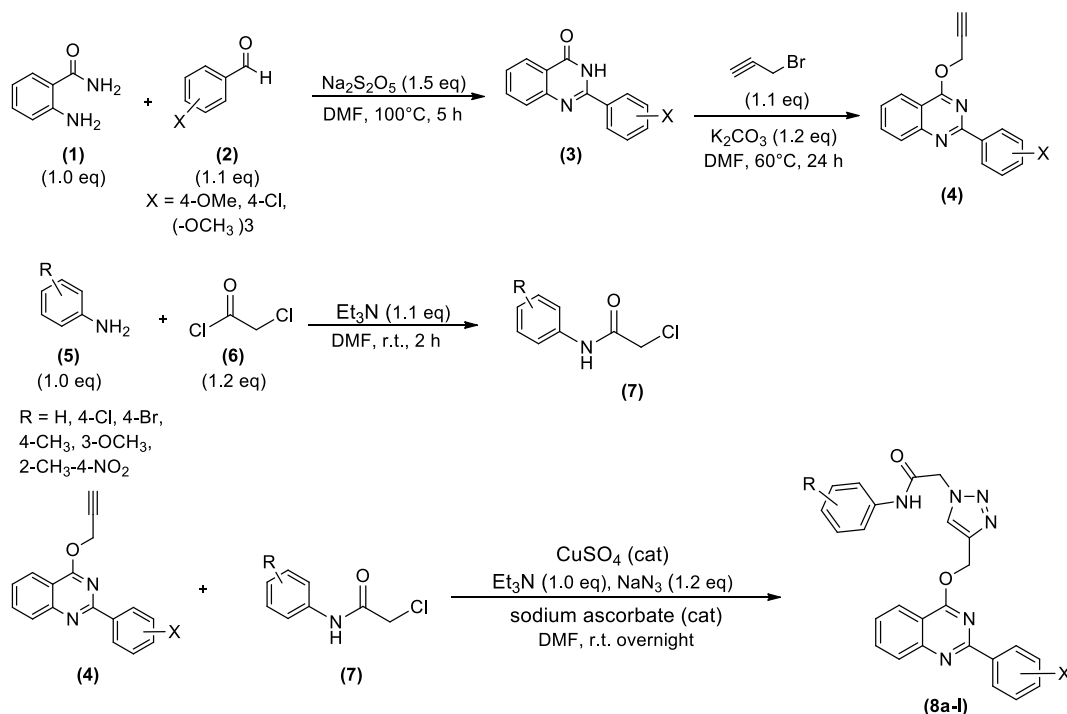


Fig. 2. Rational design of quinazoline derivatives as new anticancer agents.

cytotoxic agent. The other modification was performed by adding aryl acetamide moiety to improve the hydrogen bond features for the novel analogs with the possible target. The cytotoxic potential of derivatives was evaluated against two human cancer cell lines. Moreover, docking studies were also presented to understand the interactions between these potent derivatives and the possible target.



Scheme 1. Synthesis of the compounds **8a-l**.

2. Results and discussion

2.1. Chemistry

As shown in Scheme 1, a series of quinazolines bearing triazole-acetamide derivatives were synthesized. First, the key intermediate quinazoline derivatives (**3**) were synthesized from the reaction of 2-Aminobenzamide (**1**) and Arylaldehyde derivatives **2** in DMF. in the presence of Na₂S₂O₅. Then, compounds **3** reacted with Propargyl bromide in the presence of catalytic amounts of K₂CO₃ in DMF for 24 h to prepare 2-phenyl-4-(prop-2-yn-1-yloxy)quinazoline derivatives (**4**).

On the other hand, the reaction between different anilines (**5**) and chloroacetyl chloride (**6**) in the presence of Et₃N in DMF for 2 h gave the corresponding compound 2-chloro-*N*-phenylacetamide derivatives (**7**). Finally, the click reaction of compounds **7** and derivatives **4** led to the formation of target compounds **8a-l**.

2.2. In vitro biological activities

The new series of synthesized compounds **8a-l** were tested for their *in vitro* cytotoxic potential against HCT116 (colon), MCF-7 (breast), and HepG2 (liver) cancer cell lines plus WRL-68 (normal hepatic cell line) as negative control by using MTT (3-(4,5-dimethylthiazol-2-yl)-2,5-diphenyltetrazolium bromide) assay. The IC₅₀ values are presented in Table 1. Based on our results and considering the substituted quinazoline derivatives, structure-activity relationships (SARs) were constructed for the designed scaffold.

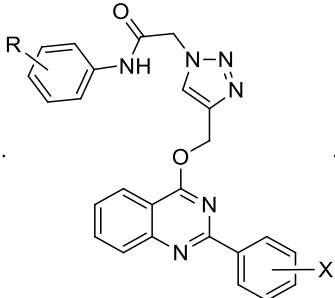
MTT evaluations of all compounds against all tested cell lines showed that the cytotoxicity of all entries after 72 h of incubation was better than 48 h, confirming the time-dependent effect of all compounds.

Cytotoxic screening against HCT-116 cells revealed that **8a** (X = 4-methoxy and R = H) was the most potent compound against HCT-116 with an IC₅₀ value of 10.72 and 5.33 μM after 47 and 72 h, respectively.

- As can be seen in compound **8b-f** (X = 4-OCH₃), substitution of electron-withdrawing groups at the R position of phenyl ring such as *para*-chlorine (**8b**) or *para*-bromine (**8c**) reduced the cytotoxic activity compared to **8a**. However, introducing the *para*-methyl group at R on the phenyl pendant (**8d**) as an electron-donating group did improve the cytotoxic potential compared to **8b** and **8c**. Replacement of *para*-methyl with *meta*-methoxy moiety significantly destroyed cytotoxic activity. Continually, the presence of multi-substitutions on the phenyl ring showed moderate to good toxicity with IC₅₀ values of 36.24 and 23.89 μM after 47 and 72 h, respectively.

Table 1

Cancer cell growth inhibitory effect of synthesized derivatives measured by MTT reduction assay in the term of IC₅₀



Compound	X	R	IC ₅₀ against HCT-116		IC ₅₀ against MCF-7 μM		IC ₅₀ against HepG2		IC ₅₀ against WRL-68	
			μM	μM	μM	μM	μM	μM	μM	μM
			48 h	72 h	48 h	72 h	48 h	72 h	48 h	72 h
8a	4-OCH ₃	H	10.72	5.33	38.06	12.96	17.48	7.94	112.49	94.07
8b	4-OCH ₃	4-Cl	77.08	68.59	25.9	20.92	78.85	19.83	107.89	89.78
8c	4-OCH ₃	4-Br	47.8	12.17	111.35	62.19	30.38	13.03	105.55	74.35
8d	4-OCH ₃	4-CH ₃	30.05	8.97	39.9	20.01	59.21	14.96	113.03	83.48
8e	4-OCH ₃	3-OCH ₃	159.6	90.59	35.19	23.04	46.03	10.18	111.92	82.71
8f	4-OCH ₃	2-CH ₃ -4-NO ₂	36.24	23.89	21.29	18.04	26.12	9.15	100.10	90.26
8g	4-Cl	H	49.21	24.5	67.18	20.9	38.79	13.24	103.07	85.10
8h	4-Cl	4-Br	42.29	41.84	34.13	20.59	90.55	8.55	115.05	89.55
8i	4-Cl	4-CH ₃	48.09	24.21	220.7	97.01	55.15	10.91	117.13	86.35
8j	4-Cl	3-Br	176.15	54.18	164.2	55.81	55.76	12.69	109.57	78.64
8k	3,4,5-tri OCH ₃	H	69.02	41.08	24.21	11.32	72.38	16.22	116.66	84.41
8l	3,4,5-tri OCH ₃	4-CH ₃	64.27	29.41	28.79	26.54	41.44	13.61	100.90	71.32
Doxorubicin ^[b]			1.66	1.21	1.15	0.82	1.96	1.31	2.19	1.73

a Data represented in terms of mean ± SD.

b positive control.

- Assessment on **8g-j** derivatives bearing 4-Cl at X position showed that **8g** (X = 4-Cl and R = H) as unsubstituted derivative in this set recorded an IC₅₀ value of 49.21 μM, which showed lower potency than **8a** counterpart, confirming the positive role of 4-methoxy at X position. However, 4-Br (**8h**) or 4-CH₃ (**8i**) substitutions did not improve the potency compared to **8g**. Similar to the previous set, introducing *meta*-moiety at R (**8j**, R = 3-Br) significantly abolished the activity.
- **8k** (X = 3,4,5-triOCH₃, R = H) and **8l** (X = 3,4,5-triOCH₃, R = 4-CH₃) exhibited almost equipotent cytotoxicity profile; however, after 72 h more reduction in IC₅₀ value was seen in **8l** (IC₅₀ = 29.41 μM) compared to **8k** (IC₅₀ = 41.08 μM).

With regards to the MCF-7 cancer cells, **8f** exhibited the best IC₅₀ value after 48 h (IC₅₀ = 21.29 μM), while the lowest IC₅₀ value came back to **8k** (IC₅₀ = 11.32 μM), followed by **8a** (IC₅₀ = 12.96 μM) after 72 h.

- Comparing the anticancer activity of **8a-f** (X = 4-OCH₃) demonstrated that **8f** possessing 2-CH₃-4-NO₂ afforded good potency with an IC₅₀ value of 21.29 after 48 h. This group's second top potent derivative was compound **8b** bearing 4-Cl at R (IC₅₀ = 25.90 μM) after 48 h. There were not significant cytotoxic differences between **8a** (X = 4OCH₃, R = H), **8d** (X = 4OCH₃, R = 4-CH₃) and **8e** (X = 4OCH₃, R = 3OCH₃) after 48 h with IC₅₀ values in the range of 35.19–39.90 in this group. Based on these results, the electron-donating groups did not show significant differences in cytotoxicity. Disappointingly, compound **8c** possessing 4-Br at R demonstrated a remarkable reduction in the cytotoxic activity (IC₅₀ = 111.35 μM).
- Also, the **8g-j** (X = 4-Cl) evaluation demonstrated that **8h** containing 4-Br at R as the electron-withdrawing group had moderate cytotoxic activity (IC₅₀ = 34.13 μM after 48 h and IC₅₀ = 20.59 μM after 72 h) in this set. However, the position replacement of *para*-bromine to *meta* (**8j**) changed the activity in such a manner that a decline in potency was seen. Also, there was a dramatic reduction in cytotoxic activity via introducing *para*-methyl at R as a moderate-electron donating group (**8i**).
- In cases of **8k** and **8l**, it was seen that the presence of 3,4,5-triOCH₃ as strong and bulky electron-donating moiety had a positive effect on cytotoxic activity.

Table 2

Molecular docking results of compounds **8a**, **8f**, and **8k** against PARP-1 (PDB ID: 4UND).

Compound	Residues	Interaction type	Moiety	Distance Å
8a	Gly894	Hydrogen Bond	Acetamide	1.95
	Arg878	Hydrogen Bond	Acetamide	1.77
	Tyr889	Hydrogen Bond	Acetamide	3.23
	Met890	Hydrogen Bond	Methoxyphenyl	2.79
	His862	Hydrogen Bond	Methoxyquinazoline	3.02
	Ala898	Hydrophobic (Pi-Alkyl)	Quinazoline	5.02
	Tyr907	Hydrophobic (Pi-Pi)	Quinazoline	3.84
	Tyr896	Hydrophobic (Pi-Pi)	Quinazoline	4.07
	Tyr896	Hydrophobic (Pi-Pi)	Methoxyphenyl	4.88
	Tyr896	Hydrophobic (Pi-Pi)	Triazole	4.66
	Ala880	Hydrophobic (Pi-Alkyl)	Phenylacetamide	4.26
	Pro881	Hydrophobic (Pi-Alkyl)	Phenylacetamide	5.22
	Gly863	Hydrogen Bond	Methoxynitrophenyl	3.32
	Ser904	Hydrogen Bond	Methoxynitrophenyl	2.30
	Tyr907	Hydrogen Bond	Acetamide	2.27
	Lys903	Hydrogen Bond	Acetamide	2.93
Met890	Hydrogen Bond	Triazole	3.11	
8f	Glu988	Hydrophobic	Acetamide	2.96
	His862	Hydrophobic	Methoxynitrophenyl	4.16
	Glu763	Hydrophobic	Methoxyquinazoline	2.96
	Tyr889	Hydrophobic	Methoxyquinazoline	3.26
	Tyr896	Hydrophobic (Pi-Pi)	Methoxynitrophenyl	5.40
	Glu763	Electrostatic (Pi-cation)	Quinazoline	3.61
	Ala762	Hydrophobic (Pi-Alkyl)	Quinazoline	3.99
	Met890	Hydrophobic (Pi-Alkyl)	Triazole	5.27
	Arg878	Hydrogen Bond	Acetamide	1.51
	Tyr896	Hydrogen Bond	Triazole	2.91
	Met890	Hydrogen Bond	Trimethoxyphenyl	3.11
	Gly878	Hydrophobic	Acetamide	2.30
	Glu763	Hydrophobic	Trimethoxyphenyl	2.98
	Gly888	Hydrophobic	Trimethoxyphenyl	2.23
	Tyr907	Hydrophobic (Pi-Pi)	Quinazoline	3.88
	8k	Tyr896	Hydrophobic (Pi-Pi)	Quinazoline
Tyr896		Hydrophobic (Pi-Pi)	Trimethoxyphenyl	4.03
Tyr889		Hydrophobic (Pi-Pi)	Trimethoxyphenyl	2.23
Arg878		Electrostatic (Pi-cation)	Phenylacetamide	5.21
Ala880		Hydrophobic (Pi-Alkyl)	Phenylacetamide	4.36
Pro881		Hydrophobic (Pi-Alkyl)	Phenylacetamide	5.40
Lys903		Hydrophobic (Pi-Alkyl)	Quinazoline	5.32
Ala898		Hydrophobic (Pi-Alkyl)	Quinazoline	4.99

- It would be interesting to note that after 72 h, **8k** showed the best activity with an IC₅₀ value of 11.32 μM followed by **8a**, **8f**, and **8h**.

The anticancer activity of all derivatives against HepG2 cells exhibited similar results compared to the HCT-116 cell line, so **8a** was the most potent agent, recording an IC₅₀ value of 17.48 and 7.94 μM after 47 and 72 h, respectively.

- As can be seen in derivatives bearing 4-OCH₃ at X position (**8a-f**), any type of substitution inferior the potencies, and amongst **8f** derivative bearing multi substitutions at X (X = 2-CH₃-4-NO₂) took the second place after **8a**.
- In the case of derivatives bearing 4-Cl at X position (**8g-j**), the IC₅₀ value in the range of 8.55–13.24 μM after 72 h were recorded. Unexpectedly, **8j** (X = 3-Br) was the active agent among **8g-j** derivatives with 8.55 μM cytotoxicity after 72 h.
- Regarding **8k** and **8l**, interesting results were seen so that these two derivatives had significant cytotoxicity after 72 h compared to 48 h.

To better understand the cytotoxic behavior of synthesized derivatives, all analogs were examined against the normal cell line, WRL-68. Assessment after 48 h showed IC₅₀ value in the range of 100.10–117.13 μM and 71.32–94.07 μM after 72 h. Interestingly, **8a** and **8f**, the most potent anticancer agents, recorded limited toxicity against normal cell line. Evaluation of all derivatives exhibited good cytotoxic activity against MOLT-4 MCF-7 and HepG2 cells with no significant effect against WRL-68 normal cells.

2.2.1. Docking

Throughout the recent few years, quinazolines and their derivatives were reported as poly (ADP-ribose) polymerase (PARP) inhibitors [40–42]. PARP is a family of proteins involved in several cellular processes, such as DNA repair, genomic stability, and programmed cell death. PARP-1 (ARTD1) is a well-characterized isoform of the PARPs family that catalyzes MARYlation and DNA repair. Developing compounds with the potency to inhibit PARP-1 is a priority in cancer therapy [43,44]. This protein consists of multi-domains, four DNA-binding domains (three Zn-fingers and one WGR domain), an auto modification domain consisting of a BRCT motif, and a catalytic domain with two important regions named the nicotinamide-ribose binding subsite and the adenosine subsite [45]. Most highly potent PARP-1 inhibitors can form interactions with the Gly863, Tyr907, Ser904, and Tyr907, and have extended substituent access to the adenosine site of the PARP-1 active site.

As a result, the molecular docking study was performed to better understand the behavior of the potent derivatives **8a**, **8f**, and **8k**, in the binding site of PARP-1 molecular docking. First, the reliability and accuracy of the applied docking protocol were assessed by re-docking the crystalized inhibitor into the enzyme's active site. The superimposed structures between the docked and the crystalized inhibitor over PARP-1 exhibited an RMSD value of 1.77 Å. A value less than 2 Å in the acceptable range.

As a result, molecular docking studies on the most potent derivatives (**8a**, **8f**, and **8k**) were performed to evaluate the binding energy and possible pose toward the active site of PARP-1. The results are presented in Table 2. **8a**, **8f**, and **8k** recorded binding energy of −12.61, −12.52, and −12.87 kcal/mol, respectively, confirming the high affinity of these compounds toward PARP-1.

As shown in Fig. 3, the quinazoline ring of compound **8a** occupied the nicotinamide-ribose binding site, which most of the potent PARP-1 inhibitors bind to. And phenylacetamide pendant properly fitted into the adenine-ribose binding site and improved the binding affinities. Similar confirmation and pose were observed in the **8k** derivative (Fig. 4). As presented in Fig. 5, **8f** inversely fitted into the binding site so that trimethoxyphenyl oriented toward nicotinamide-ribose binding site while methoxy substituted on quinazoline ring occupied adenine-ribose site.

Interestingly, all three evaluated derivatives fitted well into the pockets of PARP-1 and effectively interacted with critical residues (highlighted in red color in Table 2) of the PARP-1 binding site.

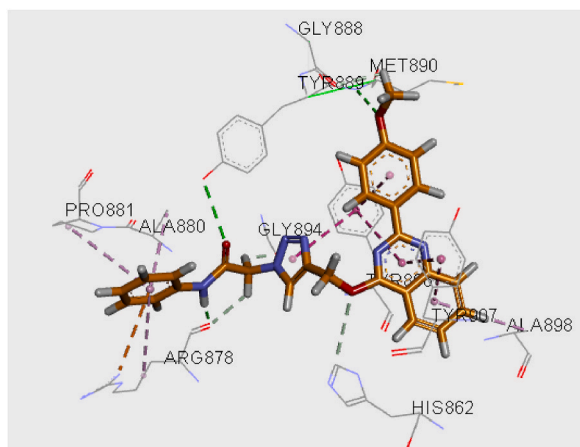


Fig. 3. Binding mode of compound **8a** in PARP-1 active site.

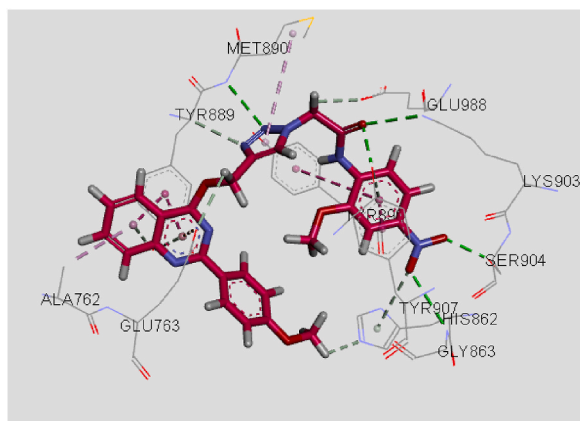


Fig. 4. Binding mode of compound **8f** in PARP-1 active site.

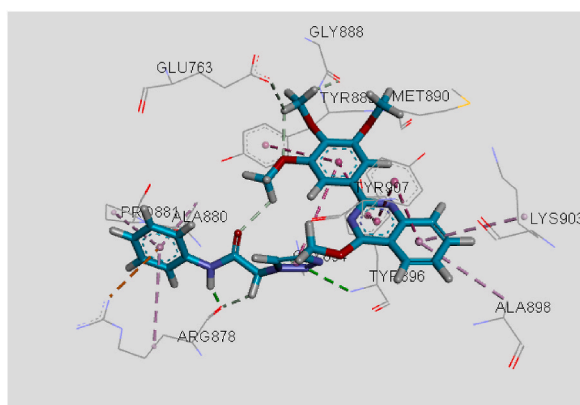


Fig. 5. Binding mode of compound **8k** in PARP-1 active site.

3. Conclusion

In this study, the hybrid structures of novel quinazoline derivatives bearing different bearing triazole-acetamides were designed and synthesized. The obtained compounds were tested for *in vitro* cytotoxic activities against three human cancer cell lines named HCT-116, MCF-7, and HepG2 after 48 and 72 h. The results implied that quinazoline-triazole-acetamide compounds exhibited moderate to good anticancer potential. The most potent derivative against HCT-116 was **8a** ($X = 4\text{-OCH}_3$ and $R = \text{H}$) with an IC_{50} value of 10.72 and 5.33 μM after 48 and 72 h. This compound also showed promising potency against HepG2 with IC_{50} values of 17.48 and 7.94 after 48 and 72 h, respectively. The cytotoxic analysis against MCF-7 showed that **8f** with $\text{IC}_{50} = 21.29 \mu\text{M}$ (48 h) exhibited the best activity, while compounds **8k** ($\text{IC}_{50} = 11.32 \mu\text{M}$) and **8a** ($\text{IC}_{50} = 12.96 \mu\text{M}$), known as the most effective cytotoxic agents after 72 h. Interestingly assessments of all derivatives against normal cell line recorded low toxicity. The obtained results of the current study disclosed the promising potencies of these derivatives in drug discovery as anticancer agents.

4. Material and method

4.1. General method for synthesis of 2-phenylquinazolin-4(3H)-one derivative (3)

The mixture of 5-Aminobenzamide **1** (1 mmol), different Aldehyde **2** (1.1 mmol) and $\text{Na}_2\text{S}_2\text{O}_5$ (1.5 mmol) was stirred in DMF at 100 °C for 5 h to produce quinazolin-4(1H)-one derivative (compound **3**).

4.2. General method for synthesis of 2-phenyl-4-(prop-2-yn-1-yloxy)quinazoline derivative (4)

Compounds **3** (1 mmol) and propargyl bromide (1.1 mmol) in the presence of K_2CO_3 (1.1 mmol) in DMF for 24 h to prepare derivatives **4**.

4.3. General method for synthesis of 2-chloro-*N*-phenylacetamide derivative (7)

2-chloro-*N*-phenylacetamide derivatives (7) were synthesized via the reaction of compound 5 (1 mmol) and Chloroacetyl chloride 6 (1.2 mmol) in the presence of Et₃N in DMF for 2 h.

4.4. General method for synthesis the substituted derivatives of *N*-phenyl-2-(4-(((2-phenylquinazolin-4-yl)oxy)methyl)-1*H*-1,2,3-triazol-1-yl)acetamide (8a-l)

The click reaction of compounds 7 (1 mmol) and quinazolines 4 (1 mmol) in presence of Et₃N (1 mmol), NaN₃ (1.2 mmol), CuSO₄ (catalytic amount), and sodium ascorbate (catalytic amount) led to the formation of target compounds 8a-l.

2-(4-(((2-(4-methoxyphenyl)quinazolin-4-yl)oxy)methyl)-1*H*-1,2,3-triazol-1-yl)-*N*-phenylacetamide (8a)

Yield 72% (335 mg), light brown solid: m.p. 218–220 °C. IR: (KBr) 3370, 1666, 1560, 1340, 1250 cm⁻¹. ¹H NMR (500 MHz, DMSO-*d*₆) δ 10.46 (s, 1H), 8.54 (dd, *J* = 9.0, 1.4 Hz, 2H), 8.35 (d, *J* = 4 Hz, 1H), 8.09 (dd, *J* = 8.1, 1.2 Hz, 1H), 7.98–7.82 (m, 2H), 7.68–7.44 (m, 3H), 7.32 (td, *J* = 9.0, 1.4 Hz, 2H), 7.18–6.91 (m, 3H), 5.89 (s, 2H), 5.35 (s, 2H), 3.85 (s, 3H). ¹³C N.M.R. (125 MHz, DMSO-*d*₆) δ 176.00, 165.48, 158.67, 157.87, 150.12, 142.89, 138.34, 132.40, 130.27, 128.58, 128.22, 127.81, 126.97, 125.97, 123.01, 121.62, 121.44, 117.44, 114.85, 65.50, 56.26, 55.28. Anal.Calcd for C₂₆H₂₂N₆O₃: C 66.94, H 4.75, N 18.02. Found: 67.12, H 4.70, N 17.89.

N-(4-chlorophenyl)-2-(4-(((2-(4-methoxyphenyl)quinazolin-4-yl)oxy)methyl)-1*H*-1,2,3-triazol-1-yl)acetamide (8b)

Yield 74% (370 mg), brown solid: m.p. 242–243 °C. IR: (KBr) 3365, 1671, 1549, 1332, 1231, 763 cm⁻¹. ¹H NMR (500 MHz, DMSO-*d*₆) δ 10.60 (s, 1H), 8.54 (d, *J* = 8.6 Hz, 2H), 8.34 (s, 1H), 8.09 (d, *J* = 8.4 Hz, 1H), 7.95–7.85 (m, 2H), 7.63–7.50 (m, 3H), 7.37 (d, *J* = 8.9 Hz, 2H), 7.10 (d, *J* = 8.7 Hz, 2H), 5.89 (s, 2H), 5.36 (s, 2H), 3.85 (s, 3H). ¹³C N.M.R. (125 MHz, DMSO-*d*₆) δ 175.94, 165.56, 158.67, 157.54, 150.06, 142.49, 138.34, 133.01, 132.40, 130.27, 129.44, 127.98, 127.08, 126.92, 122.89, 121.44, 120.58, 117.44, 114.39, 65.57, 56.26, 55.53. Anal.Calcd for C₂₆H₂₁ClN₆O₃: C 62.34, H 4.23, N 16.78. Found: 67.22, H 4.03, N 17.91.

N-(4-bromophenyl)-2-(4-(((2-(4-methoxyphenyl)quinazolin-4-yl)oxy)methyl)-1*H*-1,2,3-triazol-1-yl)acetamide (8c)

Yield 79% (429 mg), brown solid: m.p. 258–260 °C. IR: (KBr) 3349, 1658, 1569, 1325, 1212, 683 cm⁻¹. ¹H NMR (500 MHz, DMSO-*d*₆) δ 10.59 (s, 1H), 8.53 (dd, *J* = 9.0, 1.4 Hz, 2H), 8.34 (s, 1H), 8.09 (d, *J* = 8.2 Hz, 1H), 7.99–7.79 (m, 2H), 7.66–7.44 (m, 5H), 7.10 (dd, *J* = 9.0, 1.4 Hz, 2H), 5.89 (s, 2H), 5.35 (s, 2H), 3.85 (s, 3H). ¹³C N.M.R. (125 MHz, DMSO-*d*₆) δ 175.90, 165.53, 158.77, 157.64, 150.16, 142.48, 138.38, 132.57, 130.27, 129.44, 127.81, 127.08, 126.97, 122.89, 122.27, 121.89, 121.34, 117.22, 114.80, 65.57, 56.31, 55.44. Anal.Calcd for C₂₆H₂₁BrN₆O₃: C 57.26, H 3.88, N 15.41. Found: 57.42, H 3.99, N 15.53.

2-(4-(((2-(4-methoxyphenyl)quinazolin-4-yl)oxy)methyl)-1*H*-1,2,3-triazol-1-yl)-*N*-(*p*-tolyl)acetamide (8d)

Yield 70% (336 mg), light brown solid: m.p. 232–234 °C. IR: (KBr) 3363, 1650, 1578, 1319, 1262 cm⁻¹. ¹H NMR (500 MHz, DMSO-*d*₆) δ 10.36 (s, 1H), 8.54 (d, *J* = 8.7 Hz, 2H), 8.34 (s, 1H), 8.09 (d, *J* = 8.2 Hz, 1H), 7.97–7.82 (m, 2H), 7.62–7.50 (m, 1H), 7.44 (d, *J* = 8.1 Hz, 2H), 7.21–6.91 (m, 4H), 5.88 (s, 2H), 5.33 (s, 2H), 3.85 (s, 3H), 2.24 (s, 3H). ¹³C N.M.R. (125 MHz, DMSO-*d*₆) δ 175.37, 165.10, 158.09, 157.29, 150.06, 142.49, 138.70, 136.79, 132.40, 130.11, 129.44, 127.98, 126.97, 126.25, 122.27, 121.62, 121.05, 117.43, 114.39, 65.57, 56.26, 55.41, 21.26. Anal.Calcd for C₂₇H₂₄N₆O₃: C 67.49, H 5.03, N 17.49. Found: 67.30, H 4.89, N 17.67.

N-(3-methoxyphenyl)-2-(4-(((2-(4-methoxyphenyl)quinazolin-4-yl)oxy)methyl)-1*H*-1,2,3-triazol-1-yl)acetamide (8e)

Yield 73% (362 mg), light brown solid: m.p. 253–255 °C. IR: (KBr) 3356, 1661, 1565, 1343, 1241 cm⁻¹. ¹H NMR (500 MHz, DMSO-*d*₆) δ 10.42 (s, 1H), 8.53 (d, *J* = 8.7 Hz, 2H), 8.32 (s, 1H), 8.08 (d, *J* = 8.2 Hz, 1H), 7.92–7.91 (m, 2H), 7.58 (t, *J* = 8.7 Hz, 1H), 7.50 (d, *J* = 8.1 Hz, 1H), 7.36 (t, *J* = 8.6 Hz, 1H), 7.16 (d, *J* = 8.1 Hz, 1H), 7.10 (d, *J* = 8.6 Hz, 1H), 7.00 (s, 1H), 5.88 (s, 2H), 5.43 (s, 2H), 3.85 (s, 3H), 3.79 (s, 3H). ¹³C N.M.R. (125 MHz, DMSO-*d*₆) δ 175.17, 165.05, 160.21, 158.20, 157.03, 149.67, 142.88, 140.35, 132.31, 130.31, 129.55, 12.55, 127.80, 125.96, 122.62, 121.43, 117.43, 116.77, 114.47, 110.70, 110.18, 65.04, 57.91, 57.65, 57.04. Anal.Calcd for C₂₇H₂₄N₆O₄: C 65.31, H 4.87, N 16.93. Found: 65.56, H 4.69, N 16.66.

2-(4-(((2-(4-methoxyphenyl)quinazolin-4-yl)oxy)methyl)-1*H*-1,2,3-triazol-1-yl)-*N*-(2-methyl-4-nitrophenyl)acetamide (8f)

Yield 68% (357 mg), brown solid: m.p. 274–275 °C. IR: (KBr) 3370, 1675, 1553, 1356, 1206 cm⁻¹. ¹H NMR (500 MHz, DMSO-*d*₆) δ 10.34 (s, 1H), 8.54 (d, *J* = 8.6 Hz, 2H), 8.34 (s, 1H), 8.17 (s, 1H), 8.01 (d, *J* = 8.2 Hz, 1H), 7.83 (d, *J* = 8.6 Hz, 1H), 7.58 (t, *J* = 8.6 Hz, 1H), 7.44 (d, *J* = 8.7 Hz, 1H), 7.21–7.17 (m, 2H), 6.96 (d, *J* = 8.1 Hz, 2H), 5.84 (s, 2H), 5.30 (s, 2H), 3.80 (s, 3H), 2.25 (s, 3H). ¹³C N.M.R. (125 MHz, DMSO-*d*₆) δ 175.08, 166.58, 161.11, 159.29, 150.62, 146.05, 142.88, 140.35, 137.28, 134.80, 132.39, 130.26, 127.28, 125.96, 124.56, 122.10, 121.05, 120.57, 114.38, 109.68, 64.77, 56.32, 55.77, 19.72. Anal.Calcd for C₂₇H₂₃N₇O₅: C 61.71, H 4.41, N 18.66. Found: 61.47, H 4.65, N 18.78.

2-(4-(((2-(4-chlorophenyl)quinazolin-4-yl)oxy)methyl)-1H-1,2,3-triazol-1-yl)-N-phenylacetamide (8g)

Yield 81% (380 mg), brown solid: m.p. 226–228 °C. IR: (KBr) 3343, 1667, 1575, 1339, 1226, 692 cm^{-1} . ^1H NMR (500 MHz, DMSO- d_6) δ 10.45 (s, 1H), 8.60 (d, J = 8.6 Hz, 2H), 8.36 (s, 1H), 8.14 (d, J = 8.3 Hz, 1H), 8.04–7.91 (m, 2H), 7.70–7.59 (m, 3H), 7.55 (d, J = 8.0 Hz, 2H), 7.31 (t, J = 7.8 Hz, 2H), 7.07 (t, J = 7.3 Hz, 1H), 5.91 (s, 2H), 5.35 (s, 2H). ^{13}C N.M.R. (125 MHz, DMSO- d_6) δ 176.00, 166.02, 158.67, 150.16, 142.49, 140.09, 134.19, 132.40, 132.32, 129.44, 129.00, 128.56, 128.03, 127.81, 126.97, 123.01, 121.62, 121.44, 117.43, 65.05, 56.31. Anal.Calcd for $\text{C}_{25}\text{H}_{19}\text{ClN}_6\text{O}_2$: C 63.76, H 4.07, N 17.85. Found: 63.61, H 4.26, N 18.02.

N-(4-bromophenyl)-2-(4-(((2-(4-chlorophenyl)quinazolin-4-yl)oxy)methyl)-1H-1,2,3-triazol-1-yl)acetamide (8h)

Yield 85% (465 mg), brown solid: m.p. 257–259 °C. IR: (KBr) 3359, 1664, 1559, 1348, 1247, 736 cm^{-1} . ^1H NMR (500 MHz, DMSO- d_6) δ 10.57 (d, J = 24.5 Hz, 1H), 8.68–8.48 (m, 2H), 8.35 (s, 1H), 8.13 (d, J = 8.3 Hz, 1H), 8.04–7.88 (m, 2H), 7.72–7.34 (m, 6H), 7.09 (dd, J = 8.8, 1.4 Hz, 1H), 5.91 (s, 2H), 5.35 (s, 2H). ^{13}C N.M.R. (125 MHz, DMSO- d_6) δ 157.94, 165.26, 158.29, 150.16, 142.35, 137.54, 134.48, 132.87, 132.57, 131.88, 129.36, 128.58, 127.81, 126.79, 122.88, 122.36, 122.11, 121.44, 117.43, 65.83, 56.20. Anal.Calcd for $\text{C}_{25}\text{H}_{18}\text{BrClN}_6\text{O}_2$: C 54.61, H 3.30, N 15.29. Found: 54.43, H 3.36, N 15.08.

2-(4-(((2-(4-chlorophenyl)quinazolin-4-yl)oxy)methyl)-1H-1,2,3-triazol-1-yl)-N-(p-tolyl)acetamide (8i)

Yield 79% (382 mg), light brown solid: m.p. 236–238 °C. IR: (KBr) 3364, 1655, 1571, 1363, 1225, 712 cm^{-1} . ^1H NMR (500 MHz, DMSO- d_6) δ 10.37 (s, 1H), 8.60 (dd, J = 8.6, 1.4 Hz, 2H), 8.36 (s, 1H), 8.20 (d, J = 8.4 Hz, 2H), 8.15 (d, J = 7.6 Hz, 2H), 7.84 (t, J = 7.6 Hz, 1H), 7.74 (d, J = 8.2 Hz, 2H), 7.63 (d, J = 8.5 Hz, 2H), 7.53 (t, J = 7.5 Hz, 1H), 5.91 (s, 2H), 5.33 (s, 2H), 2.25 (s, 3H). ^{13}C N.M.R. (125 MHz, DMSO- d_6) δ 175.44, 165.72, 158.27, 150.25, 142.25, 136.84, 136.10, 135.23, 133.01, 132.57, 129.44, 129.23, 128.93, 127.73, 126.79, 122.89, 121.55, 121.34, 117.32, 64.61, 56.83, 20.02. Anal.Calcd for $\text{C}_{26}\text{H}_{21}\text{ClN}_6\text{O}_2$: C 64.40, H 4.37, N 17.33. Found: 64.66, H 4.74, N 17.17.

N-(3-bromophenyl)-2-(4-(((2-(4-chlorophenyl)quinazolin-4-yl)oxy)methyl)-1H-1,2,3-triazol-1-yl)acetamide (8j)

Yield 83% (454 mg), brown solid: m.p. 245–247 °C. IR: (KBr) 3352, 1652, 1557, 1330, 1217, 751 cm^{-1} . ^1H NMR (500 MHz, DMSO- d_6) δ 10.63 (s, 1H), 8.55 (d, J = 8.8 Hz, 2H), 8.34 (s, 1H), 8.09 (d, J = 5.2 Hz, 1H), 7.89 (d, J = 5.2 Hz, 1H), 7.76 (t, J = 8.1 Hz, 1H), 7.65 (d, J = 5.2 Hz, 1H), 7.59–7.57 (m, 3H), 7.50 (s, 1H), 7.37 (d, J = 8.7 Hz, 2H), 5.78 (s, 2H), 5.33 (s, 2H). ^{13}C N.M.R. (125 MHz, DMSO- d_6) δ 176.29, 165.78, 158.29, 157.48, 150.16, 142.35, 134.48, 132.57, 131.13, 130.29, 130.11, 127.89, 127.21, 126.79, 125.30, 124.29, 122.70, 121.62, 121.34, 117.32, 116.85, 56.35, 56.26. Anal.Calcd for $\text{C}_{25}\text{H}_{18}\text{BrClN}_6\text{O}_2$: C 54.61, H 3.30, N 15.29. Found: 54.45, H 3.44, N 15.10.

N-phenyl-2-(4-(((2-(3,4,5-trimethoxyphenyl)quinazolin-4-yl)oxy)methyl)-1H-1,2,3-triazol-1-yl)acetamide (8k)

Yield 80% (420 mg), brown solid: m.p. 267–269 °C. IR: (KBr) 3359, 1663, 1536, 1360, 1283, 1159 cm^{-1} . ^1H NMR (500 MHz, DMSO- d_6) δ 10.44 (s, 1H), 8.34 (s, 1H), 8.13 (d, J = 8.1 Hz, 1H), 8.01–7.85 (m, 4H), 7.62 (td, J = 8.1, 1.4 Hz, 1H), 7.55 (d, J = 8.3 Hz, 2H), 7.31 (t, J = 7.6 Hz, 2H), 7.07 (t, J = 7.4 Hz, 1H), 5.91 (s, 2H), 5.35 (s, 2H), 3.93 (d, J = 1.2 Hz, 6H), 3.75 (s, 3H). ^{13}C N.M.R. (125 MHz, DMSO- d_6) δ 175.44, 165.26, 158.56, 153.47, 150.06, 142.43, 139.28, 139.10, 132.57, 128.93, 128.09, 127.81, 126.90, 124.18, 122.89, 121.62, 121.34, 117.43, 104.71, 65.50, 56.48, 55.75, 55.26. Anal.Calcd for $\text{C}_{28}\text{H}_{26}\text{N}_6\text{O}_5$: C 63.87, H 4.98, N 15.96. Found: 63.65, H 5.14, N 15.79.

N-(p-tolyl)-2-(4-(((2-(3,4,5-trimethoxyphenyl)quinazolin-4-yl)oxy)methyl)-1H-1,2,3-triazol-1-yl)acetamide (8l)

Yield 84% (453 mg), brown solid: m.p. 277–279 °C. IR: (KBr) 3368, 1669, 1581, 1358, 1276, 1163 cm^{-1} . ^1H NMR (500 MHz, DMSO- d_6) δ 10.35 (s, 1H), 8.33 (s, 1H), 8.12 (d, J = 8.1 Hz, 1H), 8.02–7.84 (m, 4H), 7.62 (td, J = 8.2, 1.4 Hz, 1H), 7.43 (d, J = 8.1 Hz, 2H), 7.11 (d, J = 8.2 Hz, 2H), 5.90 (s, 2H), 5.32 (s, 2H), 3.93 (s, 6H), 3.75 (s, 3H), 2.24 (s, 3H). ^{13}C N.M.R. (125 MHz, DMSO- d_6) δ 175.94, 165.90, 158.34, 153.11, 149.99, 142.33, 139.20, 136.84, 135.58, 132.74, 129.23, 127.89, 126.92, 124.90, 123.01, 121.55, 121.29, 117.32, 105.06, 65.50, 56.59, 55.94, 55.35, 20.02. Anal.Calcd for $\text{C}_{29}\text{H}_{28}\text{N}_6\text{O}_5$: C 64.43, H 5.22, N 15.55. Found: 64.73, H 5.36, N 15.81.

4.5. In vitro cytotoxic evaluation

HCT-116 MCF-7, HepG2 and WRL-68 cells were obtained from Iranian Biological Resource Center, Tehran, Iran. The cells were grown in RPMI1640 medium supplemented with fetal bovine serum (FBS, 10%) and maintained at 37 °C in the presence of 5% CO_2 . The cells were seeded into 96-well micro-culture plates. After 24 h, the culture medium was replaced with a medium containing different concentrations of newly synthesized compounds. Control wells were supplemented with the same volume of growth medium without any drugs. Cells were then incubated at 37 °C for 48 or 72 h. At the end of the exposure time, the medium was removed and MTT solution 0.5 mg/ml was added to each well. The plates were incubated at 37 °C for 4 h, after which DMSO was added to each well to solubilize the formed formazan crystals and the absorbance of each well was read with a microplate reader at 570 nm. The IC_{50}

values were calculated from sigmoidal curves of percent viability plotted against the tested compounds' concentrations.

4.6. Molecular docking

The PARP-1 crystal structure has been taken from the Protein Data Bank (PDB ID: 4UND) and was docked using the Autodock software. Flexible ligand dockings were accomplished for the selected compounds. The best positions of the selected compounds against PARP-1 were chosen by analyzing the interactions between the enzyme and inhibitors. The best-scoring positions achieved by the docking score were then selected and visualized using Discovery Studio Client 2017.

Declarations

Author contribution statement

Keyvan Pedrood, Fahimeh Taayoshi, Ali Yavari, Seyed Mohammad Reza Mohajeri, Nadia Garmsiri, Vahid Haghpanah, Meysam Soleymaniabadi: Performed the experiments; Wrote the paper.

Ali Moazzam, MeySayed Mahmoud Sajjadi-Jazi, Bagher Larijani: Conceived and designed the experiments; Wrote the paper.

Aida Iraj, Haleh Hamedifar: Contributed reagents, materials, analysis tools or data; Wrote the paper.

Samira Ansari, Neda Adibpour: Analyzed and interpreted the data; Wrote the paper.

Mohammad Mahdavi: Conceived and designed the experiments; Analyzed and interpreted the data; Wrote the paper.

Funding statement

This research did not receive any specific grant from funding agencies in the public, commercial, or not-for-profit sectors.

Data availability statement

Data will be made available on request.

Declaration of interest's statement

The authors declare no conflict of interest.

Appendix A. Supplementary data

Supplementary data to this article can be found online at <https://doi.org/mmcdoino>

References

- [1] V.V. Padma, An overview of targeted cancer therapy, *Biomedicine* 5 (4) (2015) 19.
- [2] F. Bray, J. Ferlay, I. Soerjomataram, R.L. Siegel, L.A. Torre, A. Jemal, Global cancer statistics 2018: GLOBOCAN estimates of incidence and mortality worldwide for 36 cancers in 185 countries, *CA, A Cancer J. Clinicians* 68 (6) (2018) 394–424.
- [3] D. Hanahan, R.A. Weinberg, Hallmarks of cancer: the next generation, *Cell* 144 (5) (2011) 646–674.
- [4] Z. Li, X. Fu, J. Huang, P. Zeng, Y. Huang, X. Chen, C. Liang, Advances in screening and development of therapeutic aptamers against cancer cells, *Front. Cell Dev. Biol.* 9 (1225) (2021).
- [5] C.-H. Tang, G. Sethi, P.-L. Kuo, Novel medicines and strategies in cancer treatment and prevention, *BioMed Res. Int.* 2014 (2014), 474078.
- [6] S.A. Eccles, D.R. Welch, Metastasis: recent discoveries and novel treatment strategies, *Lancet* 369 (9574) (2007) 1742–1757.
- [7] C. Chakraborty, A.R. Sharma, G. Sharma, B.K. Sarkar, S.-S. Lee, The novel strategies for next-generation cancer treatment: miRNA combined with chemotherapeutic agents for the treatment of cancer, *Oncotarget* 9 (11) (2018) 10164–10174.
- [8] T.A. Yap, C.P. Carden, S.B. Kaye, Beyond chemotherapy: targeted therapies in ovarian cancer, *Nat. Rev. Cancer* 9 (3) (2009) 167–181.
- [9] B. Insuasty, H. Torres, J. Quiroga, R. Abonia, R. Rodriguez, M. Nogeras, A. Sanchez, C. Saitz, S. Alvarez, S. Zaccino, Synthesis, characterization and in vitro antifungal evaluation of novel benzimidazo [1, 2-c] quinazolines, *J. Chil. Chem. Soc.* 51 (2) (2006) 927–932.
- [10] V. Alagarsamy, R. Giridhar, M. Yadav, R. Revathi, K. Ruckmani, E. De Clercq, AntiHIV, antibacterial and antifungal activities of some novel 1, 4-disubstituted-1, 2, 4-triazolo [4, 3-a] quinazolin-5 (4 h)-ones, *Indian J. Pharmaceut. Sci.* 68 (4) (2006).
- [11] I. Khan, S. Zaib, S. Batool, N. Abbas, Z. Ashraf, J. Iqbal, A. Saeed, Quinazolines and quinazolinones as ubiquitous structural fragments in medicinal chemistry: an update on the development of synthetic methods and pharmacological diversification, *Bioorg. Med. Chem.* 24 (11) (2016) 2361–2381.
- [12] R.P. Modh, E. De Clercq, C. Pannecouque, K.H. Chikhaliya, Design, synthesis, antimicrobial activity and anti-HIV activity evaluation of novel hybrid quinazoline–triazine derivatives, *J. Enzym. Inhib. Med. Chem.* 29 (1) (2014) 100–108.
- [13] R. Rohini, P.M. Reddy, K. Shanker, A. Hu, V. Ravinder, Antimicrobial study of newly synthesized 6-substituted indolo [1, 2-c] quinazolines, *Eur. J. Med. Chem.* 45 (3) (2010) 1200–1205.
- [14] S. Jantova, Š. Stankovský, K. Špírková, In vitro antibacterial activity of ten series of substituted quinazolines, *Biologia* 59 (6) (2004) 741–752.
- [15] S.A. Khan, A.M. Asiri, H.M. Basiri, M. Asad, M.E.M. Zayed, K. Sharma, M.Y. Wani, Synthesis and evaluation of Quinoline-3-carbonitrile derivatives as potential antibacterial agents, *Bioorg. Chem.* 88 (2019), 102968.
- [16] S.A. Khan, Green synthesis, spectrofluorometric characterization and antibacterial activity of heterocyclic compound from chalcone on the basis of in vitro and quantum chemistry calculation, *J. Fluoresc.* 27 (3) (2017) 929–937.

- [17] S.A. Khan, Q. Ullah, S. Syed, Alimuddin, A.S.A. Almalki, S. Kumar, R.J. Obaid, M.A. Alsharif, S.Y. Alfaifi, H. Parveen, Microwave assisted one-pot synthesis, photophysical and physicochemical studies of novel biologically active heterocyclic Donor (D)- π -Acceptor (A) chromophore, *Bioorg. Chem.* 112 (2021), 104964.
- [18] S. Wang, X.-H. Yuan, S.-Q. Wang, W. Zhao, X.-B. Chen, B. Yu, FDA-approved pyrimidine-fused bicyclic heterocycles for cancer therapy: synthesis and clinical application, *Eur. J. Med. Chem.* 214 (2021), 113218.
- [19] G. Marzaro, A. Guiotto, A. Chilin, Quinazoline derivatives as potential anticancer agents: a patent review (2007–2010), *Expert Opin. Ther. Pat.* 22 (3) (2012) 223–252.
- [20] S. Ravez, O. Castillo-Aguilera, P. Depreux, L. Goossens, Quinazoline derivatives as anticancer drugs: a patent review (2011–present), *Expert Opin. Ther. Pat.* 25 (7) (2015) 789–804.
- [21] I. Ahmad, An insight into the therapeutic potential of quinazoline derivatives as anticancer agents, *Med. Chem. Comm.* 8 (5) (2017) 871–885.
- [22] I. Khan, A. Ibrar, W. Ahmed, A. Saeed, Synthetic approaches, functionalization and therapeutic potential of quinazoline and quinazolinone skeletons: the advances continue, *Eur. J. Med. Chem.* 90 (2015) 124–169.
- [23] R. Hanselmann, G.E. Job, G. Johnson, R. Lou, J.G. Martynow, M.M. Reeve, Synthesis of an antibacterial compound containing a 1,4-substituted 1H-1,2,3-Triazole: a scalable alternative to the "click" reaction, *Org. Process Res. Dev.* 14 (1) (2010) 152–158.
- [24] M. Mohammadi-Khanaposhtani, M. Safavi, R. Sabourian, M. Mahdavi, M. Pordeli, M. Saeedi, S.K. Ardestani, A. Foroumadi, A. Shafiee, T. Akbarzadeh, Design, synthesis, in vitro cytotoxic activity evaluation, and apoptosis-induction study of new 9 (10 H)-acridinone-1, 2, 3-triazoles, *Mol. Divers.* 19 (4) (2015) 787–795.
- [25] Y. Wang, G.L. Damu, J.-S. Lv, R.-X. Geng, D.-C. Yang, C.-H. Zhou, Design, synthesis and evaluation of clinafloxacin triazole hybrids as a new type of antibacterial and antifungal agents, *Bioorg. Med. Chem. Lett* 22 (17) (2012) 5363–5366.
- [26] M.S. Asgari, M. Mohammadi-Khanaposhtani, M. Kiani, P.R. Ranjbar, E. Zabihi, R. Pourbagher, R. Rahimi, M.A. Faramarzi, M. Biglar, B. Larijani, M. Mahdavi, H. Hamedifar, M.H. Hajimiri, Biscoumarin-1,2,3-triazole hybrids as novel anti-diabetic agents: design, synthesis, in vitro α -glucosidase inhibition, kinetic, and docking studies, *Bioorg. Chem.* 92 (2019), 103206.
- [27] M.S. Asgari, M. Mohammadi-Khanaposhtani, Z. Sharafi, M.A. Faramarzi, H. Rastegar, E. Nasli Esfahani, F. Bandarian, P. Ranjbar Rashidi, R. Rahimi, M. Biglar, M. Mahdavi, B. Larijani, Design and synthesis of 4,5-diphenyl-imidazole-1,2,3-triazole hybrids as new anti-diabetic agents: in vitro α -glucosidase inhibition, kinetic and docking studies, *Mol. Divers.* 25 (2) (2021) 877–888.
- [28] P. Silalai, S. Jaipae, J. Tocharus, A. Athipornchai, A. Suksamrarn, R. Saeng, New 1,2,3-Triazole-genipin analogues and their anti-alzheimer's activity, *ACS Omega* 7 (28) (2022) 24302–24316.
- [29] K. Sztanke, T. Tuzimski, J. Rzymowska, K. Pasternak, M. Kandefers-Szerszeń, Synthesis, determination of the lipophilicity, anticancer and antimicrobial properties of some fused 1, 2, 4-triazole derivatives, *Eur. J. Med. Chem.* 43 (2) (2008) 404–419.
- [30] B.S. Holla, B. Veerendra, M. Shivananda, B. Poojary, Synthesis characterization and anticancer activity studies on some Mannich bases derived from 1, 2, 4-triazoles, *Eur. J. Med. Chem.* 38 (7–8) (2003) 759–767.
- [31] P. Singh, R. Raj, V. Kumar, M.P. Mahajan, P. Bedi, T. Kaur, A. Saxena, 1, 2, 3-Triazole tethered β -lactam-chalcone bifunctional hybrids: synthesis and anticancer evaluation, *Eur. J. Med. Chem.* 47 (2012) 594–600.
- [32] S. Sathish Kumar, H. P. Kavitha, Synthesis and biological applications of triazole derivatives—a review, *Mini-Reviews Org. Chem.* 10 (1) (2013) 40–65.
- [33] H.W. El-Shafey, R.M. Gomaa, S.M. El-Messery, F.E. Goda, Synthetic approaches, anticancer potential, HSP90 inhibition, multitarget evaluation, molecular modeling and apoptosis mechanistic study of thioquinazolinone skeleton: promising antitumor cancer agent, *Bioorg. Chem.* 101 (2020), 103987.
- [34] A. Faraji, R. Motahari, Z. Hasanvand, T. Oghabi Bakhshaiesh, M. Toolabi, S. Moghimi, L. Firoozpour, M.A. Boshagh, R. Rahmani, S.H.M.E. Ketabforoosh, H. R. Bijanzadeh, R. Esmaili, A. Foroumadi, Quinazolin-4(3H)-one based agents bearing thiadiazole-urea: synthesis and evaluation of anti-proliferative and antiangiogenic activity, *Bioorg. Chem.* 108 (2021), 104553.
- [35] P.S.G. Nunes, G. da Silva, S. Nascimento, S.P. Mantoani, P. de Andrade, E.S. Bernardes, D.F. Kawano, A.M. Leopoldino, I. Carvalho, Synthesis, Biological evaluation and molecular docking studies of novel 1,2,3-triazole-quinazolines as antiproliferative agents displaying ERK inhibitory activity, *Bioorg. Chem.* 113 (2021), 104982.
- [36] S. Gatadi, G. Pulivendala, J. Gour, S. Malasala, S. Bujji, R. Parupalli, M. Shaikh, C. Godugu, S. Nanduri, Synthesis and evaluation of new 4(3H)-Quinazolinone derivatives as potential anticancer agents, *J. Mol. Struct.* 1200 (2020), 127097.
- [37] P.A. Plé, F. Jung, S. Ashton, L. Hennequin, R. Laine, R. Morgentin, G. Pasquet, S. Taylor, Discovery of AZD2932, a new Quinazoline Ether Inhibitor with high affinity for VEGFR-2 and PDGFR tyrosine kinases, *Bioorg. Med. Chem. Lett* 22 (1) (2012) 262–266.
- [38] M. Mahdavi, S. Dianat, B. Khavari, S. Moghimi, M. Abdollahi, M. Safavi, A. Mouradzagun, S. Kabudanian Ardestani, R. Sabourian, S. Emami, T. Akbarzadeh, A. Shafiee, A. Foroumadi, Synthesis and biological evaluation of novel imidazopyrimidin-3-amines as anticancer agents, *Chem. Biol. Drug Des.* 89 (5) (2017) 797–805.
- [39] M. Mahdavi, K. Pedrood, M. Safavi, M. Saeedi, M. Pordeli, S.K. Ardestani, S. Emami, M. Adib, A. Foroumadi, A. Shafiee, Synthesis and anticancer activity of N-substituted 2-arylquinazolinones bearing trans-stilbene scaffold, *Eur. J. Med. Chem.* 95 (2015) 492–499.
- [40] K.M. Amin, M.M. Anwar, M.M. Kamel, E.M. Kassem, Y.M. Syam, S.A. Elseginy, Synthesis, cytotoxic evaluation and molecular docking study of novel quinazoline derivatives as PARP-1 inhibitors, *Acta Pol. Pharm.* 70 (5) (2013) 833–849.
- [41] K. Magyar, L. Deres, K. Eros, K. Bruszt, L. Seress, J. Hamar, K. Hideg, A. Balogh, F. Gallyas, B. Sumegi, K. Toth, R. Halmosi, A quinazoline-derivative compound with PARP inhibitory effect suppresses hypertension-induced vascular alterations in spontaneously hypertensive rats, *Biochim. Biophys. Acta (BBA) - Mol. Basis Dis.* 1842 (7) (2014) 935–944.
- [42] R. Bansal, A. Malhotra, Therapeutic progression of quinazolines as targeted chemotherapeutic agents, *Eur. J. Med. Chem.* 211 (2021), 113016.
- [43] A.G. Thorsell, T. Ekblad, T. Karlberg, M. Löw, A.F. Pinto, L. Trésaugues, M. Moche, M.S. Cohen, H. Schüler, Structural basis for potency and promiscuity in poly (ADP-ribose) polymerase (PARP) and tankyrase inhibitors, *J. Med. Chem.* 60 (4) (2017) 1262–1271.
- [44] N.P. Karche, M. Bhone, N. Sinha, G. Jana, G. Kukreja, S.P. Kurhade, A.R. Jagdale, A.R. Tilekar, A.K. Hajare, G.R. Jadhav, N.R. Gupta, R. Limaye, N. Khedkar, B. R. Thube, J.S. Shaikh, N. Rao Irlapati, S. Phukan, G. Gole, A. Bommakanti, H. Khanwalkar, Y. Pawar, R. Kale, R. Kumar, R. Gupta, V.R. Praveen Kumar, S. Wahid, A. Francis, T. Bhat, N. Kamble, V. Patil, P.B. Nigade, D. Modi, S. Pawar, S. Naidu, H. Volam, V. Pagdala, S. Mallurwar, H. Goyal, P. Bora, P. Ahirrao, M. Singh, P. Kamalakannan, K.R. Naik, P. Kumar, R.G. Powar, R.B. Shankar, P.R. Bernstein, J. Gundu, K. Nemmani, L. Narasimham, K.S. George, S. Sharma, D. Bakhle, R.K. Kamboj, V.P. Palle, Discovery of isoquinolinone and naphthyridinone-based inhibitors of poly(ADP-ribose) polymerase-1 (PARP1) as anticancer agents: structure activity relationship and preclinical characterization, *Bioorg. Med. Chem.* 28 (24) (2020), 115819.
- [45] I.T. Kirby, M.S. Cohen, Small-molecule inhibitors of PARPs: from tools for investigating ADP-Ribosylation to therapeutics, *Activity-Based Protein Profiling* (2018) 211–231.